energy&fuels
Article
Cite This: Energy Fuels 2018, 32, 3232−3242
pubs.acs.org/EF

Detailed Compositional Characterization of the 2014 Bangladesh Furnace Oil Released into the World's Largest Mangrove Forest

Huan Chen,[†] Robert K. Nelson,[‡] Robert F. Swarthout,[§] Gary Shigenaka,[⊥] André H. B. de Oliveira,[∥] Christopher M. Reddy,[‡] and Amy M. McKenna*[,†]

[†]National High Magnetic Field Laboratory, Florida State University, 1800 East Paul Dirac Drive, Tallahassee, Florida 32310-4005, United States

[‡]Department of Marine Chemistry and Geochemistry, Woods Hole Oceanographic Institution, Woods Hole, Massachusetts 02543, United States

[§]Department of Chemistry and Environmental Science Program, Appalachian State University, Boone, North Carolina 28608, United States

[∥]Laboratory for Assessment of Organic Contaminants (LACOr), Institute of Marine Sciences-Federal University of Ceará (LABOMAR-UFC), Av. Abolição, 3207-Meireles, CEP: 60165-081 Fortaleza, CE Brazil

[⊥]Emergency Response Division, National Oceanic and Atmospheric Administration, 7600 Sand Point Way, NE, Seattle, Washington 98115, United States

Supporting Information

ABSTRACT: On December 9, 2014, ~94 000 gallons of furnace oil spilled into the Shela River in Bangladesh, a designated World Heritage Site by the United Nations Educational, Scientific and Cultural Organization. It was the largest recorded oil spill in the Sundarbans region. Visually, furnace oil appears similar to heavy fuel oil, but little is known about its composition even though it is heavily utilized worldwide. A shift in global oil production to heavier, less well-known feeds (i.e., heavy oil and bitumen) requires molecular-level knowledge for efficient response, damage assessment, and restoration in the event of any oil spill. However, little is known about the chemical composition of furnace oil in chronic and acute releases. For the first time, we catalog the molecular-level composition of a relatively unknown furnace oil collected immediately after the 2014 Bangladesh spill and compare it to a well-characterized intermediate fuel oil (IFO) spilled in Texas City, Texas (U.S.A.) in March 2014. Through a combined technique approach, we apply comprehensive two-dimensional gas chromatography (GC×GC) analysis and Fourier transform ion cyclotron resonance mass spectrometry (FT-ICR MS) to contrast the unknown furnace oil to IFO. Combined, these techniques capture the continuum of oil components and access the less volatile, highly complex non-GC amenable compounds. GC×GC analysis provides biomarker signatures that suggest the furnace oil likely originated in the Middle East and is a refined product. We further compared the furnace oil with the Arabian light crude from Middle East origin (WP681) and revealed remarkable similarities between the two oils. Simulated distillation for the furnace oil showed that 42% of the oil mass is not volatile below 478 °C (equivalent to C_{40}; the upper limit for GC-based techniques), whereas the IFO contained 38% of the total mass $>C_{40}$. Furthermore, FT-ICR MS extends the carbon number range and unlocks the molecular composition of non-GC amenable compounds. Atmospheric pressure photoionization (APPI) and electrospray ionization (ESI) FT-ICR MS resolve and identify tens of thousands of molecular formulas in each oil and report furnace oil composition similar to whole heavy crudes. To the best of our knowledge, this is the first report of the detailed compositional characterization of any furnace oil.

INTRODUCTION

On December 9, 2014 the transport tanker *Southern Star VII* released ~94 000 gallons of furnace oil into the mangrove-lined Shela River (Sundarbans, Bangladesh).[1] The Sundarbans region includes the largest contiguous mangrove forest in the world and is home to rare and protected species such as the Irrawaddy and Ganges river dolphins and the Bengal tiger. It is designated as a World Heritage Site by the United Nations Educational, Scientific and Cultural Organization (UNESCO;[1] Figure S1). Less than 3 days after the spill, the oil had spread over 350 km^2 and had reached a second river and canal network and produced black shoreline. The oil released severely contaminated the Shela and Passur River, small creeks, canals, and forest floor, which compromised the food web and threatened aquatic.[2−5] Natural degradation of this highly viscous, heavy oil will occur slowly, and residual oil will be persistent for years.[6] Earlier in 2014, the *Kirby 27706* vessel released ~168 000 gallons of intermediate fuel oils (IFOs, RMG-380) into Galveston Bay (Texas, U.S.A.), the second largest volume oil spilled in the Gulf of Mexico after the *Deepwater Horizon* oil spill in 2010.[7,8] IFOs are more viscous than most crude oils and contain a high proportion of residual oil, which leads to prolonged contamination in the environment.[9]

The term furnace oil refers to any dark, viscous residual fuel obtained by blending heavy residues from a distillation unit with lighter residues and clarified oil from a fluid catalytic

Received: December 14, 2017
Revised: January 30, 2018
Published: February 2, 2018

DOI: 10.1021/acs.energyfuels.7b03944

cracker unit. Therefore, furnace oils cover a wide range of crude oil products and blends, from relatively light number 2 (bunker A) fuel oils to heavy number 6 (bunker C) fuel oils.[8−12] Little is known on the molecular composition of the furnace oil spilled in the Sundarbans region in 2014 or how long the oil will persist in the region.[13,14] Marzan et al. isolated and characterized hydrocarbonoclastic bacteria from the contaminated site and determined the potential for degradation, but little is known about the oil chemical composition.[15] A multinational response team organized by the United Nations Environment Programme (UNEP) and the Government of Bangladesh recovered a sample of the cargo oil from the tanker shortly after the accident. Preliminary gas chromatography (GC) analysis reports a highly viscous, high boiling, degraded product due to the absence of low molecular-weight hydrocarbons (cutting oil) compounds that are readily degraded (e.g., evaporation and dissolution). The detection of 2-methyl anthracene indicates that the furnace oil contains a refined product.[14]

The first step in mitigating the impact of an oil spill is to characterize the oil based on gas chromatography, either coupled to a flame ionization detection (GC-FID) or mass spectrometer (GC-MS).[16−22] Heavy oils, however, such as heavy fuel oil (HFO) and intermediate fuel oils (IFO), challenge GC-based techniques due to the inherent low volatility of heavy, highly polar compounds that comprise a large percentage of the total mass.[9,23−25] For example, Uhler et al. analyzed geographically distinct HFO and IFOs based on GC and reported a wide range of physical and chemical properties due to the inherent polydispersity in their chemical composition, despite all being HFO or IFO.[21] However, both IFO and HFO are blended products and, not surprisingly, contain a large mass fraction of compounds above C_{40} from refinery residues that are blended with lighter distillates, and GC can only access a subset of the total composition of these oils.[24−26] FT-ICR MS, however, extends the carbon number range (up to C_{120}) without the volatility limitations characteristic of GC-based techniques.[27−30] High boiling, heavy crude oil fractions challenge nearly all analytical techniques, and only FT-ICR MS can provide compositional characterization at the level of elemental composition assignment and provides access to high-boiling compounds.[28,30−35]

As global oil production shifts to heavier crudes and blended feedstocks, the likelihood of accidental spills increases worldwide as heavier products are transported from remote areas of the world to local refineries and power plants.[36] The highly active, constant tanker traffic and plans to construct new industrial facilities in the Sundarbans region require a robust chemical inventory of furnace oil to provide effective remediation, planning, spill response, and restoration efforts to protect the sensitive ecosystems. To the best of our knowledge, we detail the first molecular-level, comprehensive characterization of furnace oil spilled into the marine ecosystem derived. Through bulk elemental analysis combined with advanced analytical characterization, comprehensive two-dimensional gas chromatography (GC×GC) analysis and FT-ICR MS, we juxtapose furnace oil spilled in Bangladesh to IFO spilled in Texas City to detail furnace oil composition.

EXPERIMENTAL METHODS

Sample Description. Furnace oil (Bangladesh furnace oil) was provided by the National Ocean and Atmospheric Administration. To the best of our knowledge, the sample was collected from the tanker on 12/14/14 (5 days after the spill) and received on 12/31/14. Source oil from the Texas City oil spill (hereafter IFO) was graciously provided by Prof. Edward Overton (Louisiana State University).

Elemental Analysis. Bulk elemental analysis of Bangladesh furnace oil and Texas City IFO was measured on a Thermo Finnigan Elemental Analyzer (FLASH EA 112; San Jose, CA). Complete experimental methods can be found in the Supporting Information (SI).

Viscosity. The viscosity measurement was performed on a microVISC viscometer (RheoSense Inc., CA, U.S.A.) at 25 °C.

High-Temperature Simulated Distillation (HTSD). HTSD was performed by Triton Analytics Corporation (Houston, TX, U.S.A.) according to ASTM method D7169.[37] HTSD is a GC-based technique that utilizes flame ionization detection (FID) to determine the weight percent of an oil as a function of boiling point.[38] This method provides the mass fraction that is volatile within a boiling point range (cut point interval) and can be readily applied to determine the distribution of boiling point cuts in a crude oil (up to ~C108).[38−41]

GC×GC-FID and GC×GC-TOF MS Analysis. Texas City IFO and Bangladesh furnace oil were analyzed by GC×GC-FID and GC×GC-TOF MS as previously described.[17] Chromatographic peaks were tentatively identified based on retention times in both dimensions and mass spectral matches (above 80% similarity; NIST/EPA/NIH 05 Mass Spectral Library). See the SI for complete methods.

FT-ICR MS. All solvents used were HPLC grade (JT Baker Chemical Co., Centre Valley, PA, U.S.A.). Approximately 1 mg of oil was dissolved in 1 mL of toluene to prepare a stock solution (1 mg/mL) that was further diluted to 100 μg/mL for positive ion atmospheric pressure photoionization (APPI) and 500 μg/mL for electrospray ionization (ESI) FT-ICR MS analysis spiked with 4% (by volume) formic acid (positive mode)[42] or 0.25% (by volume) tetramethylammonium hydroxide (CAS no. 75-59-2, TMAH, 25% by weight in methanol, negative mode) to ensure efficient protonation/deprotonation. Mass spectra were calibrated with custom-built software (MIDAS).[43] Peak assignments and data visualization were performed with PetroOrg software.[44] Ionization source conditions and detailed FT-ICR MS experimental conditions are provided in the SI.

RESULTS AND DISCUSSION

The most critical bulk properties characteristics of a crude oil or refined product are viscosity, density, API gravity, elemental composition, and boiling-point distribution.[36] Table 1 summarizes the bulk property comparison for the two oils. Unfortunately, there was no sufficient furnace oil sample for density and viscosity measurements for the furnace oil.

Kinematic Viscosity. Kinematic viscosity is the ratio of the absolute viscosity to the density and is traditionally used to

Table 1. Elemental Analysis (C, H, N, O, and S Weight Percent) and Bulk Property Comparison of Furnace Oil and IFO

	furnace oil	IFO
carbon (% wt)	85.9[a] ± 1.31[b]	87.1 ± 0.40
hydrogen (% wt)	11.2 ± 0.18	10.5 ± 0.02
nitrogen (% wt)	0.2 ± 0.01	0.4 ± 0.07
sulfur (% wt)	2.39 ± 0.02	0.67 ± 0.07
oxygen (% wt)	0.73 ± 0.03	0.91 ± 0.02
kinematic viscosity[c] (mm^2/s)		157.0
density[d] (kg/m^3)		977.3
API gravity°,[e]		13.2

[a]Average weight percent by mass. [b]Standard deviation based on quadruplicate measurements. [c]ASTM D445 kinematic viscosity, cSt at 50 °C. [d]ASTM D4052 at 15 °C [e]ASTM D4052, API gravity at 60 °F (15.5 °C). [f]ASTM D664.

classify marine fuels. The viscosity of Texas City IFO is 157 mm^2/s at 50 °C which suggest that it can be classified as IFO 180 (intermediate fuel oil with a maximum viscosity of 180) according to ISO 8217.[36]

Density. Density measurements provide a rough estimation of the content of a particular petroleum fluid at a standard temperature, reported as grams per cubic centimeter.[36] Marine fuels must have a density that allows them to be separated from the water during purification process before use. The density for IFO is 0.9773 g/m^3 at 15 °C (Table 1) which is similar to a standard intermediate fuel oil (ISO 8217, IFO 380, RMG 35).

API Gravity. American Petroleum Institute (API) gravity is another parameter to measure the density of liquid petroleum products relative to water. The lower the density of the oil, the higher its API gravity, which suggests the petroleum product contains more lower-boiling fractions (i.e., the Macondo source oil with an API gravity of about 37 is considered a light oil).[45,46] In this study, the API gravity of Texas IFO is measured at 13.2. Heavy (low API gravity) are more resistant to dispersion.[46]

Elemental Analysis. Table 1 shows elemental weight percentage differences in carbon, hydrogen, nitrogen, and oxygen for the furnace oil and IFO. Typically, IFOs contain low percentages of sulfur, nitrogen, and oxygen compounds, although IFO 180 and IFO 380 can have a maximum sulfur content of 3.5% according to ISO 8217. The IFO contains nearly twice the amount of nitrogen compared to the furnace oil (0.4 ± 0.07 and 0.2 ± 0.01, respectively), with slightly higher oxygen content in IFO (0.91 ± 0.02) relative to furnace oil (0.73 ± 0.03). Sulfur content, however, is over three times higher in the furnace oil (2.39 ± 0.002) compared to the IFO (0.67 ± 0.07). Sulfur presents a host of challenges for upgrading of heavy crude oil due to its recalcitrance, and combustion of sulfur-rich fuels is linked to increased mortality and morbidity in local regions.[47,48] Sulfur must be removed prior to refining strategies through hydrodesulfurization to minimize sulfur dioxide emissions that occur in combustion reactions with organic sulfur.[49−53]

Boiling Point Distribution by Simulated Distillation. The assessment of boiling points that constitute any petroleum fluid released into the environment is instrumental for determination of the distillate yields to design remediation strategies.[36,50,54] One way to determine the boiling point distribution of a crude oil is to run a simulated distillation to determine the type, content, and amount of distillate fractions, critical to ascertain the long-term impact on marine ecosystems.[28,37,55,56] Figure 1 shows the boiling point distribution recovered as a function of oven temperature for both oils. Less than ~7% of the total mass of furnace oil is recovered at 350 °C compared to ~25% for the IFO. As the oven temperature increases (400 °C), 36% of the IFO is recovered but only 14% of the furnace oil. At an oven temperature of 459 °C, half of the mass of IFO is recovered, whereas half of the furnace oil is not recovered until 502 °C. Therefore, the majority of the compounds for both samples are not volatile below 400 °C, the upper temperature limit of most traditional GC columns.[29]

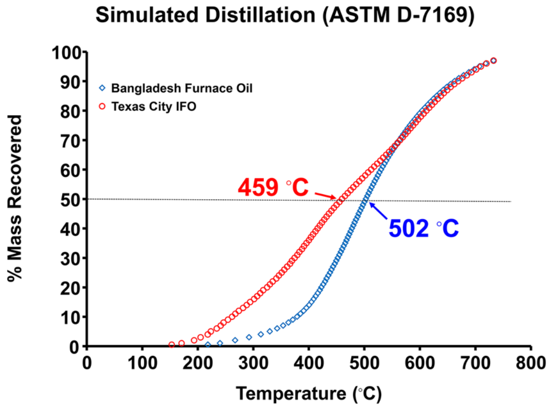

Figure 1. Simulated distillation for Bangladesh furnace oil and IFO from Texas City obtained according to ASTM D-7169, showing percentage removed as a function of temperature. The black dashed line indicates the temperature at which half of the mass for each oil was recovered, 459 °C for the IFO and higher at 502 °C for the furnace oil. The boiling range for the furnace oil obtained through gas chromatography (GC) distillation reveals that less than 40% of IFO and less than 30% of furnace oil compounds have boiling points below 400 °C, the upper-limit for GC-based techniques.

GC×GC. GC×GC has many advantages over conventional 1D GC, specifically higher peak capacity that increases the signal-to-noise ratio and orthogonal separation that groups chemical classes into distinct regions in the two-dimensional chromatographic plane, and has been applied to petroleum characterization in both oil production and oil spill research.[16,24,45,56−58] Figure 2 shows GC×GC-FID chromatograms for furnace oil (top) and IFO (bottom). Briefly, compounds separated based on volatility in the first dimension (x axis), labeled based on elution of pure n-alkane standards and separated by relative polarizability in the second dimension (y axis). Branched isoprenoid and normal alkanes elute first in the second dimension and group along the x axis (bottom of the chromatogram). Polar, aromatic compounds are retained by the second-dimension column and elute after alkanes (top of the chromatogram). The furnace oil contains an abundance of alkanes between C$_{22}$−C$_{36}$ and a low proportion of aromatic compounds compared to the more aromatic IFO with majority of alkanes between C$_8$−C$_{18}$ due to its intrinsic blended nature (Figure 2b). In addition, the cumulative total mass recovered from the simulated distillation is overlaid on the GC×GC chromatogram, further highlighting that ~53% of the total mass of material contains compounds that can be accessed by GC×GC (up to C$_{38}$), and 60% of IFO compounds are accessed by GC×GC. Therefore, ~42% of the furnace oil compounds and 38% of IFO compounds are not volatile below 478 °C (equivalent to C$_{40}$) and are thus undetected in GC techniques.

Biomarker Fingerprinting. Environmental and petroleum geochemistry studies rely mainly on analysis of petroleum biomarkers, in particular individual steranes and pentacyclic triterpanes (e.g., hopanes) are particularly useful for the differentiation of crude oils and the characterization, fingerprinting, and monitoring of the degradation processes. Steranes and hopanes are natural organic compounds that are highly resistant to degradation under environmental conditions produced by ancient organisms (eukaryotes and prokaryotes correspondingly) millions of years ago. Figure 3 shows enlarged inset GC×GC-FID chromatograms of the biomarker region from (a) Bangladesh furnace oil and (b) Texas City IFO. Both of these refined petroleum spills contain common and unique biomarkers (Figures S2 and S3) that can aid source identification of the released product. List of biomarkers abbreviations, names, formulas, and atomic mass data are provided in Table S1.

Hopanoids. For example, the Texas City IFO and Bangladesh furnace oil both contain a suite of hopanoids that

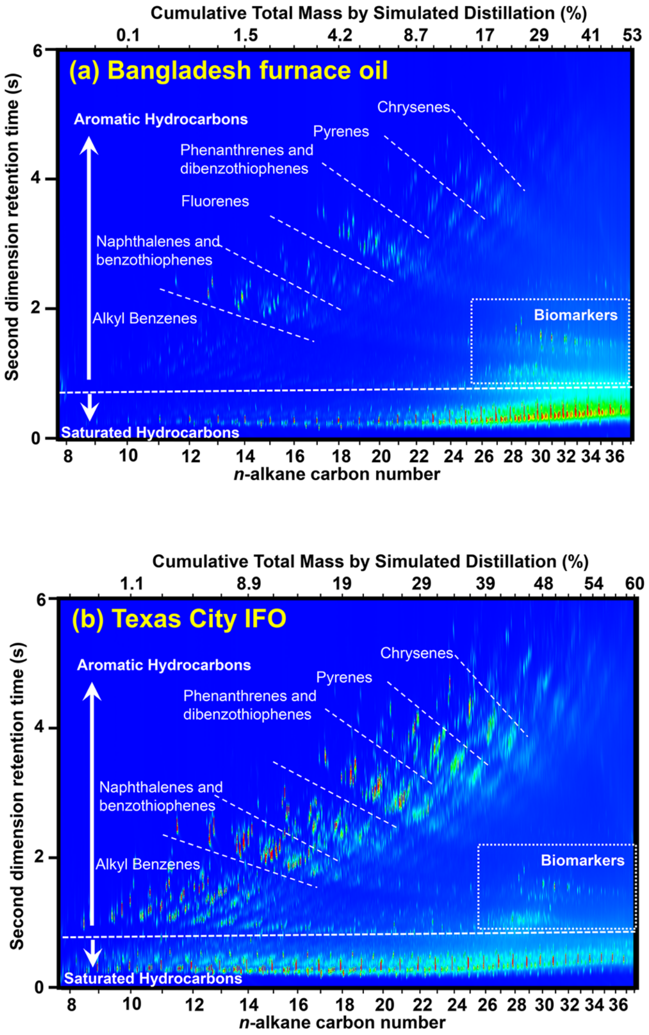

Figure 2. GC×GC chromatogram of Bangladesh furnace oil (top) and Texas City IFO (bottom) with distinct chemical classes highlighted. The data is displayed as color-contour plots, with blue representing low signal, white representing medium signal, and red representing high signal. A volatility-based separation produced a boiling point separation on the x axis and a polarity-based separation on the y axis. The furnace oil (top) collected from the tanker shortly after the 2014 Bangladesh spill and Texas City IFO (bottom) were analyzed without prior fractionation. Thus, naphthalenes, fluorenes, phenanthrenes, pyrenes, and chrysenes are observed, which are removed in silica gel fractionation routinely performed prior to GC×GC analysis. Overlayed along the top x axis is the percent mass recovered from simulated distillation as a function of n-alkane distribution. For the furnace oil, only 53% of compounds are detectable by GC×GC; for the IFO, only 60% of compounds are volatile within the GC window.

are commonly found in crude oils worldwide. The Texas City IFO also contains 25-norhopanoids, 8,14-secohopanoids, and robust sesquiterpenoids. The presence of 25-norhopanoids suggests that the refinery feedstock for this IFO may have included crude oil from a reservoir that was severely biodegraded.[59,60] The presence of a suite of 8,14-secohopanoids in the Texas City IFO provides further evidence of a biodegraded petroleum feedstock as these compounds are frequently found in biodegraded crude oils, asphalts, and bitumens.[59,61−63]

Methyl Hopanoids. In addition to the suite of normal hopanes, methylhopanoid analogs, likely derived from cyanobacteria, are identified in the Bangladesh furnace oil.[64] The methyl hopanoids are tentatively identified as 2α-methyl-hopanoids based upon (a) elution position relative to the normal hopanes and (b) mass spectral similarities to 2α-methyl-hopanoids (Figures 3 and S2).[64] The presence of 2α-methyl-hopanoids combined with a robust 17α(H),21β(H)-30-norhopane peak (NH) with an NH/H ratio of greater than 1.2 and 17α(H),21β(H)-29-norhomohopane (29-nor-HH) point to the Middle East as the origin of the Bangladesh furnace oil.

Comparison to Light Crude. To explore similarities and or differences between the furnace oil spilled in Bangladesh and crude oil from the Middle East, a light crude oil from Saudi Arabia was also analyzed. Figure 4 is a side by side comparison of Arabian Light Crude (The United States Environmental Protection Agency's standard reference material, WP681) and Bangladesh furnace oil that shows a striking similarity between the hopanoid biomarkers released during the Sundarbans Bangladesh spill and the EPA Arabian Light Crude standard (EPA WP681). Biomarkers are molecular fossils derived from the remains of deceased organisms that provide information about the source of the organic carbon in petroleum forming sediments/source rocks along with clues to the depositional environment (what the environmental conditions were like during sedimentary deposition and burial).[59] Biomarkers also chronicle molecular diagenesis transformations and provide information about the thermal history of a crude oil as biomarker molecules rearrange to more stable configurations during geologic heating. Biomarkers can also provide information about the geologic age of a crude oil, for example; flowering plant biomarkers such as oleanane may be present in crudes younger than 65 million years but are absent in preangiospermogenesis age crude oils. Thus, varying depositional environments (marine, tidal, and lacustrine) combined with varying diagenesis, burial, and geologic heating (thermal maturity transformations) regimes produce unique biomarker profiles which are of great forensic value in differentiating petroleum sources worldwide.[65]

Hopanoids. A quantitative comparison of thirty-two hopanoid and 2α-methyl-hopanoid biomarker ratios (Figure S4) highlights the similarities between the furnace oil hopanoids and these same compounds in Arabian Light Crude. 2α-Methyl-Ts coeluted with an unknown compound in both the furnace oil and the EPA WP681 standard. This unknown compound was not found in the Texas City IFO, and thus the presence of the unknown in both the furnace oil and Arabian Light Crude provides further evidence that the origin of the furnace oil was from the Middle East.

Norhopanes. The presence of C_{29}-Ts is worth discussing in the context of measuring norhopane, also present and abundant in the furnace oil. C_{29}-Ts and norhopane generally coelute on 30 m GC columns and many oil spill researchers inadvertently integrate both of these peaks together yielding erroneously high norhopane concentrations. This compromises the comparison of ratios of both norhopane and C_{29}-Ts with all other biomarker compounds. Figure S5 shows an enlarged view of a GC×GC-FID chromatogram of Bangladesh furnace oil and highlights the chromatographic resolution between NH and C_{29}-Ts. Although GC×GC expands the analytical window beyond conventional GC, by increasing peak capacity approximately 10-fold, the high proportion of compounds heavier than n-C_{40} highlights the necessity of using complementary techniques to analyze the remaining oil content.

DOI: 10.1021/acs.energyfuels.7b03944
Energy Fuels 2018, 32, 3232−3242

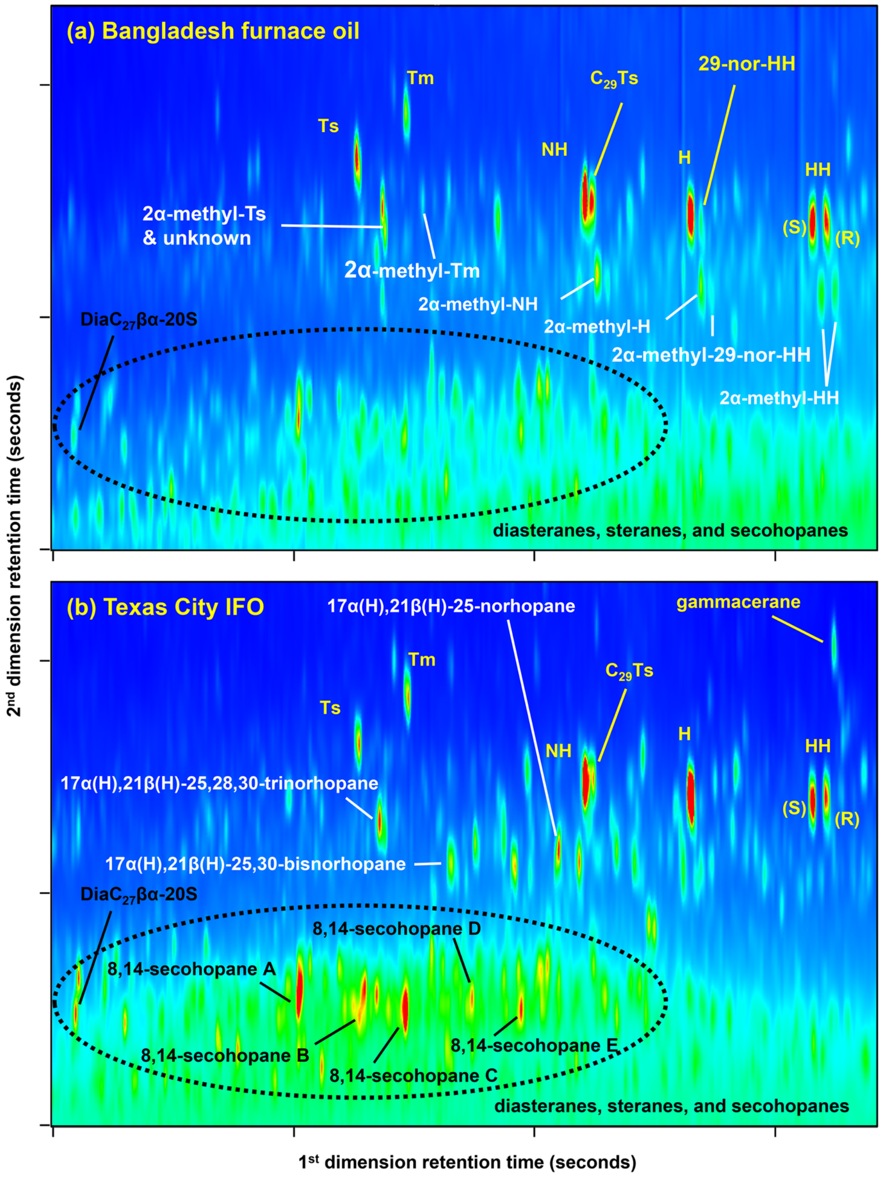

Figure 3. Enlargement of the biomarker region of the GC×GC-FID chromatogram of Bangladesh furnace oil (top) and Texas City IFO (bottom) with distinct regions annotated for several biomarker classes, including diasteranes, steranes, and hopanes. Labeled peaks include hopane and 2*α*-methyl hopane series, C_{27}-diasterane (Dia$C_{27}\beta\alpha$-20S), and 8,14-secohopane in the furnace oil. See text.

Molecular Characterization of Furnace Oil and IFO Requires Ultrahigh Resolution FT-ICR MS. APPI. APPI produces protonated and radical cations from nonpolar and polar compounds simultaneously and when coupled to FT-ICR MS has been applied to heavy crude oils, its refinery residues, asphaltenes, and deposits.[30,33−35,66−70] Figure S6 shows broadband positive-ion APPI FT-ICR mass spectra of the Texas City IFO (Figure S6a) and Bangladesh furnace oil (Figure S6b) with absorption-mode resolving power of 1 500 000 at m/z 500 that is sufficient to resolve and identify more than ~21 000 mass spectral peaks (each with signal magnitude greater than six-times the baseline noise level) in the IFO and ~34 00 peaks in the furnace oil ($200 < m/z < 1100$).[71,72] The previous characterization of heavy distillates shows that, as the boiling point increases, the molecular weight distribution shifts to higher molecular weight.[30,54,73−75] However, both the IFO and furnace oil contain a wide range of compounds of varying boiling points and span approximately the molecular weight distribution. For the blended IFO, a bimodal distribution occurs between m/z 250 and 450 that corresponds to the low boiling, more aliphatic cutting oil, and the more aromatic, higher boiling residue between m/z ~350 and 950. However, the furnace oil distribution ranges from $\sim 250 < m/z < 1000$, centered at m/z 425, in agreement with previous reports of whole heavy crudes. A slight increase in compositional complexity occurs in the furnace oil, which contains more higher boiling compounds compared to the IFO, and correspond to higher molecular weight species.[73] The molecular distribution of furnace oil indicates that its composition resembles a whole, heavy crude oil, rather than the blended IFO; however, the presence of 2-methyl anthracene by GC analysis indicates a refined product.[14]

Heteroatom Class Distribution. Ionization in APPI produces radical cations and protonated ions from aromatic functionalities and is well-suited for heavy boiling crudes and blended oils.[24,52,76,77] Figure 5 shows the heteroatom class

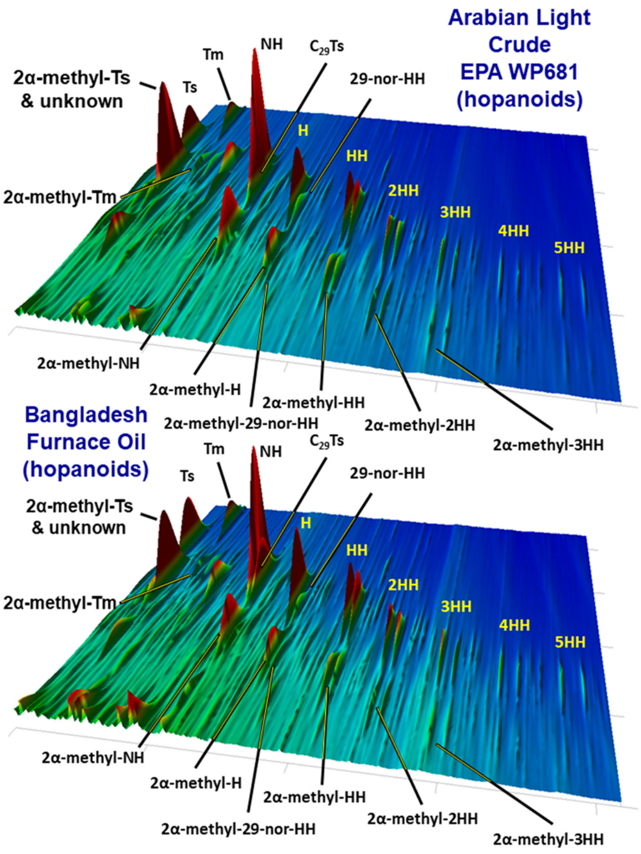

Figure 4. GC×GC-FID chromatogram for Arabian Light Crude standard (EPA WP681) and Bangladesh furnace oil enlarged for the hopanoid region that highlights the similar biomarker profiles, which indicates that the furnace oil originated from the Middle East.

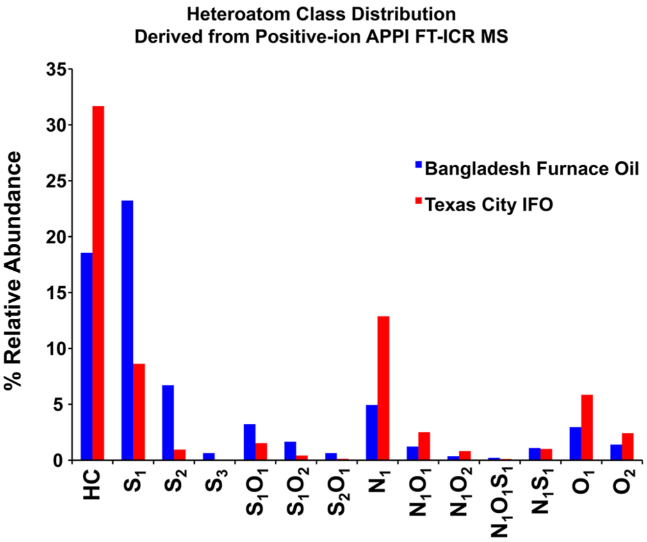

Figure 5. Heteroatom class distribution (heteroatom content) for Bangladesh furnace oil and Texas City IFO derived from positive-ion APPI FT-ICR MS. HC denotes molecules containing only hydrogen and carbon.

distribution for all detected species of >0.25% relative abundance in the APPI FT-ICR mass spectra for the furnace oil and IFO. Compounds containing a single S atom were the most abundant in the furnace oil, whereas hydrocarbon compounds were the most abundant in the IFO, as expected since furnace oil contains more than three times the mass of sulfur (by weight) than IFO, followed by hydrocarbons and S_2. Multiheteroatomic compounds, such as S_1O_1 and S_1O_2, and oxygen-containing polar species have higher boiling points due to increased intermolecular attraction and therefore are enriched in high boiling, heavy crudes. Heavy crudes and bitumens are rich in sulfur-containing species, with heteroatom class distributions similar to the furnace oil.[30,33] The higher relative abundance of sulfur-containing classes and lower relative abundance of nitrogen-containing corroborate the results of bulk elemental analysis in Table 1.

Hydrogen Deficiency versus Carbon Number. The tens of thousands of elemental compositions obtained from FT-ICR MS can be rapidly visualized in three-dimensional isoabundance color-contoured plots of carbon number versus double bond equivalents (DBE, the number of rings plus double bonds to carbon DBE = C − $h/2$ + $n/2$ + 1, calculated from each elemental composition, $C_cH_hN_nO_oS_s$)[78] or hydrogen-to-carbon ratio calculated from the neutral elemental composition.[29,35] Figure 6 shows DBE (left) and H/C ratio (right) versus carbon number from elemental compositions determined by APPI FT-ICR MS for members of the hydrocarbon, S_1, S_2, and O_1 classes in each oil. Conversion of elemental compositions derived from APPI FT-ICR MS to DBE or H/C ratio provides rapid visualization and comparison of the aromaticity (DBE) and degree of hydrogen deficiency (H/C ratio) of compounds within a heteroatom class. Relative abundance-weighted average carbon number, DBE, and H/C ratio derived from neutral elemental compositions obtained for molecular ions are shown for each class. For a given carbon number, aromaticity for polyaromatic hydrocarbons (PAHs) cannot exceed a maximum value that increases linearly with higher carbon number as shown by the red dashed line in each panel.[79,80]

Hydrocarbons. The relative-abundance weighted average DBE and carbon number for hydrocarbon (HC) compounds in both samples are fairly similar, with both samples containing an average C_{40}−C_{41} and DBE 15 (furnace oil) and DBE 16 (IFO). However, the most HC abundant compounds in the furnace oil (denoted by red arrows) contain a range of DBE values (8−16) across C_{30}−C_{36} similar to a whole Middle Eastern crude oil, whereas IFO counterparts have a more narrow DBE range (15−16) across C_{25}−C_{26} similar to products that contain cutting oils and residues (e.g., HFO).[24,33] The bimodal distribution in the IFO corresponds to the cutting oil (more aliphatic, higher H/C ratio) and the heavy distillate (more aromatic, lower H/C ratio), whereas the furnace oil spans similar compositional space as heavy crudes.[30,33]

Sulfur. For S_1 compounds in both samples, the most abundant compounds contain C_{40} with DBE 14 (furnace oil) and 15 (IFO). Two regions of high relative abundance (hot spots) appear in the furnace oil between C_{27}−C_{33} at DBE 6 and DBE 9−15, which correspond to benzothiophene (DBE 6), dibenzothiophene (DBE 9), and dinaphthothiophene (DBE 15) core structures with alkylsubstitution. DBE 10−15 likely correspond to cyclohexane and cycloalkane intercalated analogues. Compounds that contain a single sulfur in the IFO of highest relative abundance correspond to DBE 15, and C_{22}−C_{23} and correspond to condensed aromatic rings with minimal alkylation compared to IFO counterparts. As noted for the HC class, the most abundant S_1 compounds in the furnace oil contain a range of DBE (6−15) values across ~C_{28}−C_{34}, whereas the most abundant S_1 in IFO have narrow DBE values (15−17) and C_{25}−C_{28}. Compounds that contain two sulfurs

DOI: 10.1021/acs.energyfuels.7b03944
Energy Fuels 2018, 32, 3232−3242

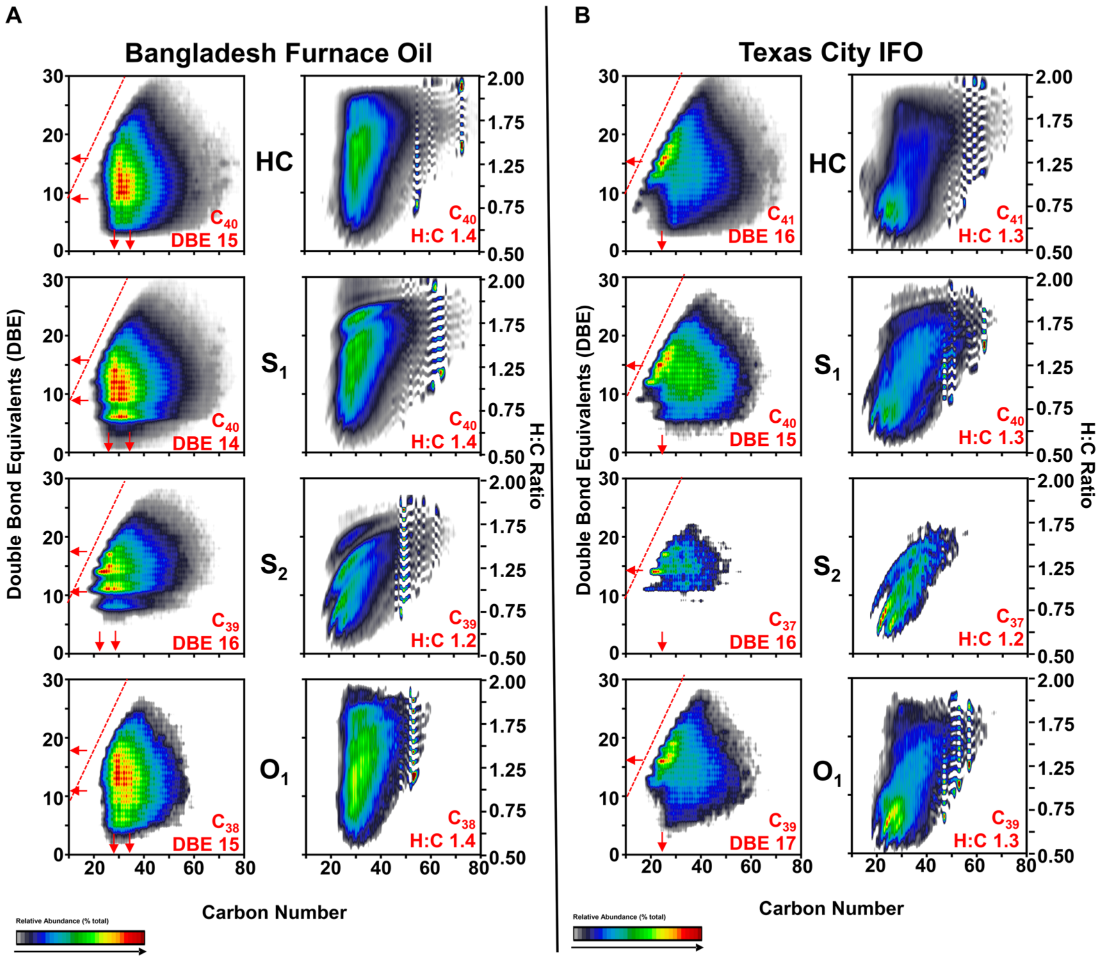

Figure 6. Isoabundance-contoured plots of double bond equivalents (DBE, left) and H:C ratio (right) versus carbon number for hydrocarbons (HC), S_1, S_2, and O_1 classes obtained from positive-ion APPI FT-ICR MS for (a) Bangladesh furnace oil and (b) IFO from Texas City. Relative abundance-weighted averaged DBE, H:C ratio, and carbon numbers calculated from neutral elemental compositions are shown in red for each heteroatom class.

(S_2) are less abundant in the IFO as noted in bulk elemental analysis (Table 1) and heteroatom class distribution (Figure 5) for both oils contain DBE 16 across a similar carbon number range but are less abundant in the IFO.

Test of the Boduszynski Continuum. Because petroleum composition is continuous in carbon number, heteroatom content, and aromaticity as a function of boiling point, crude oils that are distillate products can be identified from whole crudes based on compositional trends.[30,33,54,73−75,81,82] Briefly, each addition of a heteroatom from hydrocarbon to S_1 or N_1 or O_1 results in a decreased of 2−3 carbons per molecule to remain in the same boiling point range (i.e., defined distillation ranges). Therefore, comparison of the carbon number of highest relative abundance for hydrocarbons to S_1 would decrease if the sample was a distilled product, as previously reported.[8] However, no decrease in carbon number occurs from hydrocarbons to S_1, which indicates that neither sample is solely the result of distillation (i.e., a product with a defined upper and lower boiling point; Figure 6). However, GC analysis indicates that the furnace oil is a refined product due to the presence of 2-methyl anthracene, with a composition similar to Middle Eastern heavy crude oil based on APPI FT-ICR MS.[14,33]

Acidic Speciation by Negative-Ion ESI FT-ICR MS. Polar species, in particular, acidic compounds, are potentially water-soluble and therefore environmentally relevant to assess oil spill toxicity.[83−89] Acidic compounds, specifically the carboxylic acids, represent the most polar fraction of crude oil and are therefore the least volatile. With the increase in carbon number, volatility for compounds with carboxylic acid moieties decreases, and characterization relies on electrospray ionization that can generate quasi-molecular ions through protonation and deprotonation reactions.[90,91] Figure S7 shows the heteroatom class distribution for acidic species derived from negative-ion ESI FT-ICR MS analysis for the two samples. Modification of a conventional ESI solvent system with tetramethylammonium hydroxide (TMAH) significantly increases the compositional coverage for weakly acidic and neutral species in crude oil.[92] The most abundant compound class detected by negative-ion ESI for both oils correspond to pyrrolic nitrogen (N_1), followed by O_1 in the IFO and hydrocarbons (HC) in the furnace oil. Sulfur classes (N_1S_1) and S_1 are more abundant in the furnace oil than IFO, in agreement with previous reports on Middle Eastern crudes.

Aromaticity versus Carbon Number and H/C Ratio. Figure S8 shows isoabundance color coded contoured plots of DBE and H/C ratio versus carbon number for the acidic hydrocarbons (HC), pyrrolic nitrogen (N_1), phenols (O_1), and carboxylic acids (O_2) for both samples. Relative-abundance

DOI: 10.1021/acs.energyfuels.7b03944
Energy Fuels 2018, 32, 3232−3242

weighted averages are labeled for each class in red, in addition to the planar stability limit (red dashed line).

Five-Member Ring Hydrocarbons. Five-membered ring fused to flanking six-member aromatic hydrocarbon rings (e.g., C-9 in fluorine) can be deprotonated in TMAH-modified solvent systems.[29,92] The most abundant five-member ring hydrocarbons in the IFO correspond to DBE = 12 at C_{20} and DBE 15 at C_{24}, likely benzofluorene and dibenzofluorene structures.[92] A single hot spot occurs in the furnace oil at DBE 15 and C_{24}, with alkylsubstitution detected up to C_{60} in both samples.

Pyrrolic Nitrogen. The most abundant compounds in the IFO and furnace oil contain one nitrogen (N_1) and correspond to five-membered ring (pyrrolic) nitrogen, the most recalcitrant nitrogen compound class reported in petroleum refining and upgrading.[93−95] Pyrrolic nitrogen, in particular, has lower reactivity than sulfur counterparts and therefore increased recalcitrance in the environment.[95] Pyrrolic nitrogen compounds in both samples contain relative abundance-weighted average carbon number (C_{39}−C_{40}) and DBE (16) with carbon number distributions up to C_{60}.

Phenols Carboxylic Acids. Phenolic compounds are deprotonated and more efficiently ionized in negative-ion ESI with TMAH solvent modification. The most abundant members of the O_1 class in the furnace oil contain C_{39} with an average DBE = 15, corresponding to an H/C ratio of 1.5. Compounds that contain a single oxygen in the furnace oil correspond to two structural groups: aromatic furans with high DBE values that approach the planar stability limit and aliphatic phenolic compounds at low DBE.[80] At DBE = 4, which could correspond to four-cyclic biomarker compounds (e.g., sterane or diasteranes), the most abundant compounds occur at C_{26}, C_{28}, C_{30}, C_{32}, C_{34}, and C_{36} and likely indicate C_{26} steranes with varying length alkylsubstitution.

Carboxylic Acids. The O_2 class identified by negative ESI FT-ICR MS for crude oil corresponds to the most polar chemical functional group, the carboxylic acids. Both the furnace oil and IFO contain O_2 compounds across a range of carbon numbers and DBE values from 1 (fatty acids) to 20−25. The blended IFO contains a higher abundance of O_2 compounds compared the furnace oil and indicates a polar, acid rich residue to create the blended product. One area of high abundance in the furnace oil corresponds to C_{28} at DBE 8, which could correspond to hopanoic acid.

Nitrogen Speciation: Pyridinic versus Pyrrolic Nitrogen. Electrospray ionization selectively targets polar compounds through protonation and deprotonation reactions and speciates pyridinic versus pyrrolic nitrogen based on polarity.[27] Figure S9 shows pyridinic nitrogen (N_1, top) detected by positive-ion ESI compared to the pyrrolic nitrogen (N_1, bottom, negative ESI) for both samples. For pyridinic nitrogen compounds native to the furnace oil (top, left), the relative-abundance weighted average carbon number (C_{41}) and DBE (15) convert to an average H:C ratio of 1.4, and IFO basic nitrogen contain C_{53} and DBE 17 (H:C ratio 1.5). These compounds likely correspond to dibenzoacridine-type compounds (DBE 16) and its analogs. Figure S9 (bottom) highlights the five-member ring nitrogen compounds selectively targeted in negative-ion ESI FT-ICR MS. Furnace oil and IFO pyrrolic N_1 compounds contain approximately the same weighted average carbons per compound with DBE between 12 and 15, which correspond to benzocarbazole structures.

CONCLUSIONS

Here, we present the first molecular-level characterization of furnace oil released into the environment in 2014 and compare bulk properties and composition to an IFO spilled within the same year. Furnace oil contains more than 3.5 times the amount of sulfur compared to IFO and is more similar in bulk elemental composition to whole, heavy crude. Compounds that had boiling points above 500 °C comprise more than half the total mass of the furnace oil, whereas half the mass of IFO was volatile at 450 °C. Both oils contain a high proportion of non-GC-amenable compounds that are accessible by FT-ICR MS coupled to APPI and ESI ionization. Comprehensive GC×GC MS to identify biomarker signature in furnace oil and comparison to Arabian Light crude standard indicates that the furnace oil origin is from the Middle East. We catalogue a suite of biomarkers for the furnace oil spilled in Bangladesh to provide future studies to track and identify this oil from other spilled sources. FT-ICR mass spectral analysis extends the characterization to more 55 000 nonpolar aromatic and polar compounds. Compositional complexity in Bangladesh furnace oil converts to a ∼ 60% increase in the number of mass spectral peaks detected and assigned across the same molecular weight range (200−1000 m/z) compared to IFO. The most abundant heteroatom class in the furnace oil corresponded to sulfur-containing compounds that spanned a wide carbon number and aromaticity range similar to bitumen and heavy crudes. Furthermore, the blended nature of HFOs and IFOs creates bimodality in molecular composition that can be visualized in DBE vs. carbon number image and was not observed in the furnace oil. GC identification of 2-methyl anthracene indicates that the furnace oil contains some fraction of a refined product, and FT-ICR MS confirms that it is not a true distilled product. Collectively, these results converge on furnace oil composition similar to heavy whole crude from the Middle East rather than a blended product, important to mitigate the impact of future spills with proper and efficient remediation strategies.

ASSOCIATED CONTENT

Supporting Information

The Supporting Information is available free of charge on the ACS Publications website at DOI: 10.1021/acs.energy-fuels.7b03944.

Materials and methods including elemental analysis, GC×GC-FID and GC×GC-TOF MS analysis, and FT-ICR MS analysis. Additional results as depicted in Figures S1−S9 and Table S1. (PDF)

AUTHOR INFORMATION

Corresponding Author

*Phone: +1 850 644 4809. Fax: +1 850 644 1366. E-mail: mckenna@magnet.fsu.edu.

ORCID

Amy M. McKenna: 0000-0001-7213-521X

Notes

The authors declare no competing financial interest.

ACKNOWLEDGMENTS

The authors thank Christopher L. Hendrickson and John P. Quinn for design and maintenance of the 9.4 T instrument, Gregory T. Blakney and Yuri E. Corilo for software capabilities, and Mr. Jie Lu for helpful discussions. This work was supported by NSF Division of Materials Research through DMR-1157490, OCE-1333148, The Gulf of Mexico Research Initiative (GoMRI SA 16-30), and the State of Florida. Data are publicly available through the Gulf of Mexico Research Initiative & Data Cooperative (GRIIDC) at https://data.gulfresearchinitiative.org.

REFERENCES

(1) Alexander, C. After Oil Spill, Unique Mangrove Forest Faces More Threats. http://news.nationalgeographic.com/2015/05/150507-sundarbans-india-bangladesh-oil-spill-royal-bengal-tiger-irrawaddy-dolphin-bay-of-bengal/ (May 7, 2015).

(2) Islam, N.; Shafi, M. *Sustainable eco-tourism as a practical site management policy?: a case study on the Sundarbans world heritage site in Bangladesh*; AH Development Pub. House: Distributor, Mohiuddin & Sons: 2003.

(3) France-Presse, A. UN sends team to clean up Sunderbans oil spill in Bangladesh; The Guardian, 18 December, 2014.

(4) Chowdhury, A. H.; Mannan, M.; Gosh, P.; Akbar, M. Draft report of the research impact of oil spillage on the environment of Sundarbans (world largest mangrove forest) in Bangladesh. In 2016.

(5) Mahmud, I. Oil spill in Sundarbans threatens food cycle. *Prothom Alo* **2014**.

(6) Islam, M. M.; Hossain, M. M. Community Dependency on the Ecosystem Services from the Sundarbans Mangrove Wetland in Bangladesh. In *Wetland Science*; Springer: Berlin, 2017; pp 301−316.

(7) Yin, F.; Hayworth, J. S.; Clement, T. P. A Tale of Two Recent Spills—Comparison of 2014 Galveston Bay and 2010 Deepwater Horizon Oil Spill Residues. *PLoS One* **2015**, *10* (2), e0118098.

(8) Koolen, H. H.; Swarthout, R. F.; Nelson, R. K.; Chen, H.; Krajewski, L. C.; Aeppli, C.; McKenna, A. M.; Rodgers, R. P.; Reddy, C. M. Unprecedented insights into the chemical complexity of coal tar from comprehensive two-dimensional gas chromatography mass spectroscopy and Fourier transform ion cyclotron resonance mass spectrometry. *Energy Fuels* **2015**, *29*, 641.

(9) Abdul, J.; Abdul, G.; Han, Y.; Brignoli, O.; Telalovic, S.; Elbaz, A. M.; Im, H. G.; Roberts, W. L.; Sarathy, S. M. Heavy fuel oil pyrolysis and combustion: Kinetics and evolved gases investigated by TGA-FTIR. *J. Anal. Appl. Pyrolysis* **2017**, *127*, 183−195.

(10) Hwang, H.-M.; Stanton, B.; McBride, T.; Anderson, M. J. Polycyclic aromatic hydrocarbon body residues and lysosomal membrane destabilization in mussels exposed to the Dubai Star bunker fuel oil (intermediate fuel oil 380) spill in San Francisco Bay. *Environ. Toxicol. Chem.* **2014**, *33* (5), 1117−1121.

(11) Khosla, D. K.; Gupta, S. K.; Saraf, D. N. Multi-objective optimization of fuel oil blending using the jumping gene adaptation of genetic algorithm. *Fuel Process. Technol.* **2007**, *88* (1), 51−63.

(12) Downs, C. A.; Richmond, R. H.; Mendiola, W. J.; Rougee, L.; OStrander, G. K. Cellular physiological effects of the MV Kyowa Violet fuel-oil spill on the hard coral, Porites Iobata. *Environ. Toxicol. Chem.* **2006**, *25* (12), 3171−3180.

(13) Yousefinejad, S.; Aalizadeh, L.; Honarasa, F. Applciation of ATR-FTIR spectroscopy and chemometrics for the discrimination of furnace oil. gas oil and mazut oil. *Anal. Methods* **2016**, *8* (23), 4640−4647.

(14) Nelson, R. K.; Aeppli, C.; Arey, J. S.; Chen, H.; de Oliveira, A. H.; Eiserbeck, C.; Frysinger, G. S.; Gaines, R. B.; Grice, K.; Gros, J. Applications of Comprehensive Two-Dimensional Gas Chromatography (GC× GC) in Studying the Source, Transport, and Fate of Petroleum Hydrocarbons in the Environment. In *Standard Handbook Oil Spill Environmental Forensice*, 2nd ed.; Stout, S. A., Wang, Z., Eds.; Elsevier: London, U.K., 2016; pp 399−444.

(15) Marzan, L. W.; Sultana, T.; Hasan, M. M.; Mina, S. A.; Islam, M. R.; Rakibuzzaman, A.; Khan, M. I. H. Characterization of furnace oil bioremediation potential of hydrocarbonoclastic bacteria isolated from petroleum contaminated sites of the Sundarbans, Bangladesh. *Journal of Genetic Engineering and Biotechnology* **2017**, *15*, 103.

(16) Lemkau, K. L.; Peacock, E. E.; Nelson, R. K.; Ventura, G. T.; Kovecses, J. L.; Reddy, C. M. The M/V CoscoBusan spill: Source identification and short-term fate. *Mar. Pollut. Bull.* **2010**, *60* (11), 2123−2129.

(17) Frysinger, G. S.; Gaines, R. B.; Reddy, C. M. GC X GC - A new analytical tool for environmental forensics. *Environ. Forensics* **2002**, *3* (1), 27−34.

(18) Li, M.; Cheng, D.; Pan, X.; Dou, L.; Hou, D.; Shi, Q.; Wen, Z.; Tang, Y.; Achal, S.; Milovic, M.; Tremblay, L. Characterization of petroleum acids using combined FT-IR, FT-ICR-MS and GC-MS: Implications for the origin of high acidity oils in the Muglad Basin. *Org. Geochem.* **2010**, *41* (9), 959−965.

(19) Ventura, G. T.; Raghuraman, B.; Nelson, R. K.; Mullins, O. C.; Reddy, C. M. Compound class oil fingerprinting techniques using comprehensive two-dimensional gas chromatography (GC x GC). *Org. Geochem.* **2010**, *41* (9), 1026−1035.

(20) Wardlaw, G. D.; Arey, J. S.; Reddy, C. M.; Nelson, R. K.; Ventura, G. T.; Valentine, D. L. Disentangling oil weathering at a marine seep using GC X GC: Broad metabolic specificity accompanies subsurface petroleum biodegradation. *Environ. Sci. Technol.* **2008**, *42*, 7166−7173.

(21) Uhler, A. D.; Stout, S. A.; Douglas, G. S. Chemical heterogeneity in modern marine residual fuel oils. *Oil Spill Environmental Forensics* **2007**, 327−348.

(22) Radovic, J. R.; Aeppli, C.; Nelson, R. K.; Jimenez, N.; Reddy, C. M.; Bayona, J. M.; Albaiges, J. Assessment of photochemical processes in marine oil spill fingerprinting. *Mar. Pollut. Bull.* **2014**, *79* (1−2), 268−77.

(23) Ansell, D.; Dicks, B.; Guenette, C.; Muller, T.; Santner, R.; White, I. *A review of the problems posed by spills of heavy fuel oils*; International Oil Spill Conference, 2001; American Petroleum Institute: Washington, DC, 2001; pp 591−596.

(24) Lemkau, K. L.; McKenna, A. M.; Podgorski, D. C.; Rodgers, R. P.; Reddy, C. M. Molecular evidence of heavy-oil weathering following the M/V *Cosco Busan* spill: Insights from Fourier transform ion cyclotron resonance mass spectrometry. *Environ. Sci. Technol.* **2014**, *48*, 3760−3767.

(25) Corilo, Y. E.; Podgorski, D. C.; McKenna, A. M.; Lemkau, K. L.; Reddy, C. M.; Marshall, A. G.; Rodgers, R. P. Oil Spill Source Identification by Principal Component Analysis of Electrospray Ionization Fourier Transform Ion Cyclotron Resonance Mass Spectra. *Anal. Chem.* **2012**, *85*, 9064.

(26) Raha, S. Fate of Oil Pollution in Bangladesh-A Review. *Asian Journal of Multidisciplinary Studies* **2015**, 3 (5).

(27) Rodgers, R. P.; Schaub, T. M.; Marshall, A. G. Petroleomics: MS Returns to its Roots. *Anal. Chem.* **2005**, *77* (1), 20A.

(28) Chen, H.; Hou, A.; Corilo, Y. E.; Lin, Q.; Lu, J.; Mendelssohn, I. A.; Zhang, R.; Rodgers, R. P.; McKenna, A. M. 4 years afer the Deepwater Horizon spill: Molecular transformation of Macondo well oil in Louisiana salt marsh sediments revealed by FT-ICR mass spectrometry. *Environ. Sci. Technol.* **2016**, *50* (17), 9061−9069.

(29) McKenna, A. M.; Nelson, R. K.; Reddy, C. M.; Savory, J. J.; Kaiser, N. K.; Fitzsimmons, J. E.; Marshall, A. G.; Rodgers, R. P. Expansion of the analytical window for oil spill characterization by ultrahigh resolution mass spectrometry: beyond gas chromatography. *Environ. Sci. Technol.* **2013**, *47* (13), 7530−9.

(30) McKenna, A. M.; Purcell, J. M.; Rodgers, R. P.; Marshall, A. G. Heavy petroleum composition. 1. Exhaustive compositional analysis of Athabasca bitumen HVGO distillates by Fourier transform ion cyclotron resonance mass spectrometry: a definitive test of the Boduszynski model. *Energy Fuels* **2010**, *24* (5), 2929−2938.

(31) Qian, K.; Robbins, W. K.; Hughey, C. A.; Cooper, H. J.; Rodgers, R. P.; Marshall, A. G. Resolution and Identification of 3000 Crude Acids in Heavy Petroleum by Negative-Ion Microelectrospray High Field Fourier Transform Ion Cyclotron Resonance Mass Spectrometry. *Energy Fuels* **2001**, *15*, 1505−1511.

(32) Qian, K.; Rodgers, R. P.; Hendrickson, C. L.; Emmett, M. R.; Marshall, A. G. Reading chemical fine print: resolution and identification of 3000 nitrogen-containing aromatic compounds from

a single electrospray ionization Fourier transform ion cyclotron resonance mass spectrum of heavy petroleum. *Energy Fuels* **2001**, *15* (2), 492−498.

(33) McKenna, A. M.; Blakney, G. T.; Xian, F.; Glaser, P. B.; Rodgers, R. P.; Marshall, A. G. Heavy Petroleum Composition. 2. Progression of the Boduszynski Model to the Limit of Distillation by Ultrahigh-Resolution FT-ICR Mass Spectrometry. *Energy Fuels* **2010**, *24*, 2939−2946.

(34) McKenna, A. M.; Marshall, A. G.; Rodgers, R. P. Heavy Petroleum Composition. 4. Asphaltene Compositional Space. *Energy Fuels* **2013**, *27* (3), 1257−1267.

(35) McKenna, A. M.; Donald, L. J.; Fitzsimmons, J. E.; Juyal, P.; Spicer, V.; Standing, K. G.; Marshall, A. G.; Rodgers, R. P. Heavy petroleum composition. 3. Asphaltene aggregation. *Energy Fuels* **2013**, *27*, 1246−1256.

(36) Speight, J. *Handbook of petroleum analysis*; John Wiley & Sons Inc.: New York, 2001.

(37) ASTM, D. 7169-05. Standard Test Method for Boiling Point Distribution of Samples with Resid such as Crude Oils and Atmospheric Resids by High Temperature Gas Chromatography. *2005 ASTM Annual Book of Standards* 2005.

(38) Villalanti, D. C.; Raia, J. C.; Maynard, J. B. High-temperature Simulated Distillation Applications in Petroleum Characterization. *Encyclopedia Anal. Chem.* **2006**, 10.1002/9780470027318.a1819.

(39) Bruno, T. J. Improvements in the Measurement of Distillation Curves. 1. A Composition-Explicit Approach. *Ind. Eng. Chem. Res.* **2006**, *45* (12), 4371−4380.

(40) Smith, B. L.; Bruno, T. J. Advanced distillation curve measurement with a model predicitive temperature controller. *Int. J. Thermophys.* **2006**, *27* (5), 1419−1434.

(41) Ha, H. Z.; Ring, Z.; Liu, S. Data Reconciliation Among PIONA, GC-FIMS, and SimDis Measurements for Petroleum Fractions. *Pet. Sci. Technol.* **2008**, *26*, 7−28.

(42) Ruddy, B. M.; Huettel, M.; Kostka, J. E.; Lobodin, V. V.; Bythell, B. J.; McKenna, A. M.; Aeppli, C.; Reddy, C. M.; Nelson, R. K.; Marshall, A. G.; Rodgers, R. P. Targeted petroleomics: analytical investigation of Macondo well oil oxidation products from Pensacola Beach. *Energy Fuels* **2014**, *28* (6), 4043−4050.

(43) Blakney, G. T.; Hendrickson, C. L.; Marshall, A. G. Predator data station: A fast data acquisition system for advanced FT-ICR MS experiments. *Int. J. Mass Spectrom.* **2011**, *306* (2−3), 246−252.

(44) Corilo, Y. E. *PetroOrg. Software*, 13.2; Florida State University: Tallahassee, FL, 2017.

(45) Reddy, C. M.; Arey, J. S.; Seewald, J. S.; Sylva, S. P.; Lemkau, K. L.; Nelson, R. K.; Carmichael, C. A.; McIntyre, C. P.; Fenwick, J.; Ventura, G. T.; Van Mooy, B. A. S.; Camilli, R. Composition and fate of gas and oil released to the water column during the Deepwater Horizon oil spill. *Proc. Natl. Acad. Sci. U. S. A.* **2012**, *109*, 20229.

(46) Atlas, R. M.; Hazen, T. C. Oil biodegradation and bioremediation: A tale of the two worst spills in U.S. history. *Environ. Sci. Technol.* **2011**, *45*, 6709−6715.

(47) Kan, H.; Wong, C.-M.; Vichit-Vadakan, N.; Qian, Z. Short-term association between sulfur dioxide and daily mortality: the Public Health and Air Pollution in Asia (PAPA) study. *Environ. Res.* **2010**, *110* (3), 258−264.

(48) Saranjampour, P.; Armbrust, K. L.; Marx, B. D. Assessing the hydroxyl radical and volatilization roles in aquatic fate estimationf of sulfur heterocycles: Dibenzothiophene derivatives. *Environ. Toxicol. Chem.* **2017**, *36* (8), 1998.

(49) Agarwal, P.; Sharma, D. K. Comparative studies on the biodesulfurization of crude oil with other desulfurization techniques and deep desulfurization through integrated processes. *Energy Fuels* **2010**, *24* (1), 518−524.

(50) Altgelt, K. H.; Boduszynski, M. M. *Composition and Analysis of Heavy Petroleum Fractions*; CRC Press: New York, 1994.

(51) Liu, P.; Shi, Q.; Chung, K. H.; Zhang, Y.; Pan, N.; Zhao, S.; Xu, C. Molecular Characterization of Sulfur Compounds in Venezuela Crude Oil and Its SARA Fractions by Electrospray Ionization Fourier Transform Ion Cyclotron Resonance Mass Spectrometry. *Energy Fuels* **2010**, *24* (9), 5089−5096.

(52) Purcell, J. M.; Juyal, P.; Kim, D.-G.; Rodgers, R. P.; Hendrickson, C. L.; Marshall, A. G. Sulfur Speciation in Petroleum: Atmospheric Pressure Photoionization or Chemical Derivatization and Electrospray Ionization Fourier Transform Ion Cyclotron Resonance Mass Spectrometry. *Energy Fuels* **2007**, *21* (5), 2869−2874.

(53) Wu, Z. G.; Rodgers, R. P.; Marshall, A. G. Comparative compositional analysis of untreated and hydrotreated oil by electrospray ionization Fourier transform ion cyclotron resonance mass spectrometry. *Energy Fuels* **2005**, *19* (3), 1072−1077.

(54) Boduszynski, M. M.; Altgelt, K. H. Composition of Heavy Petroleums. 3. An Improved Boiling Point-Molecular Weight Relation. *Energy Fuels* **1992**, *6* (1), 68−72.

(55) Edwards, B. R.; Reddy, C. M.; Camilli, R.; Carmichael, C. A.; Longnecker, K.; Van Mooy, B. A. S. Rapid microbial respiration of oil from the Deepwater Horizon spill in offshore surface waters of the Gulf of Mexico. *Environ. Res. Lett.* **2011**, *6* (3), 035301.

(56) Hall, G. J.; Frysinger, G. S.; Aeppli, C.; Carmichael, C. A.; Gros, J.; Lemkau, K. L.; Nelson, R. K.; Reddy, C. M. Oxygenated weathering products of Deepwater Horizon oil come from surprising precursors. *Mar. Pollut. Bull.* **2013**, *75* (1−2), 140−149.

(57) Aeppli, C.; Carmichael, C. A.; Nelson, R. K.; Lemkau, K. L.; Graham, W. M.; Redmond, M. C.; Valentine, D. L.; Reddy, C. M. Oil weathering after the Deepwater Horizon disaster led to the formation of oxygenated residues. *Environ. Sci. Technol.* **2012**, *46* (16), 8799−8807.

(58) Carmichael, C. A.; Arey, J. S.; Graham, W. M.; Linn, L. J.; Lemkau, K. L.; Nelson, R. K.; Reddy, C. M. Floating oil-covered debris from Deepwater Horizon: identification and application. *Environ. Res. Lett.* **2012**, *7*, 015301.

(59) Peters, K. E.; Walters, C. C.; Moldowan, J. M. *The Biomarker Guide, Second ed.. I. Biomarkers and Isotopes in the Environment and Human History*; Cambridge University Press: New York, 2005; Vol. *1*.

(60) Eglinton, G.; Calvin, M. Chemical Fossils. *Sci. Am.* **1967**, *216* (1), 32−43.

(61) Frysinger, G. S.; Gaines, R. B. Separation and identification of petroleum biomarkers by comprehensive two-dimensional gas chromatography. *J. Sep. Sci.* **2001**, *24*, 87−96.

(62) Cortes, J. E.; Rincon, J. M.; Jaramillo, J. M.; Philp, R. P.; Allen, J. Biomarkers and compound-specific stable carbon isotope of n-alkanes in crude oils from Eastern Llanos Basin, Colombia. *J. South Am. Earth Sci.* **2010**, *29* (2), 198−213.

(63) Sharipova, N. S.; Budnikov, G. K.; Uspenskii, B. V.; Kayukova, G. P. Detection of biomarkers in the organic matter of rocks from the Romashkinskoe oil field using gac chromatography-mass spectrometry. *J. Anal. Chem.* **2010**, *65* (5), 438−444.

(64) Farrimond, P.; Talbot, H.; Watson, D.; Schulz, L.; Wilhelms, A. Methylhopanoids: molecular indicators of ancient bacteria and a petroleum correlation tool. *Geochim. Cosmochim. Acta* **2004**, *68* (19), 3873−3882.

(65) Wang, Z.; Stout, S. *Oil spill environmental forensics: fingerprinting and source identification*; Elsevier: Amsterdam, The Netherlands, 2010.

(66) McKenna, A. M.; Purcell, J. M.; Rodgers, R. P.; Marshall, A. G. Identification of vanadyl porphyrins in a heavy crude oil and raw asphaltene by atmospheric pressure photoionization Fourier transform ion cyclotron resonance (FT-ICR) mass spectrometry. *Energy Fuels* **2009**, *23* (4), 2122−2128.

(67) Kim, S.; Stanford, L. A.; Rodgers, R. P.; Marshall, A. G.; Walters, C. C.; Qian, K.; Wenger, L. M.; Mankiewicz, P. Microbial Alteration of the Acidic and Neutral Polar NSO Compounds in Petroleum Revealed by Fourier Transform Ion Cyclotron Resonance Mass Spectrometry. *Org. Geochem.* **2005**, *36*, 1117−1134.

(68) Klein, G. C.; Kim, S.; Rodgers, R. P.; Marshall, A. G. Mass spectral analysis of apshaltenes. I. Compositional Differences between pressure-drop and solvent-drop asphaltenes determine by electrospray ionization Fourier transfrom ion cyclotron resonance mass spectrometry. *Energy Fuels* **2006**, *20*, 1965−1972.

(69) Mapolelo, M. M.; Rodgers, R. P.; Blakney, G. T.; Yen, A. T.; Asomaning, S.; Marshall, A. G. Characterization of naphthenic acids in crude oils and naphthenates by electrospray ionization FT-ICR mass spectrometry. *Int. J. Mass Spectrom.* **2011**, *300* (2−3), 149−157.

(70) Marshall, A. G.; Beu, S. C.; Blakney, G. T.; Hendrickson, C. L.; McKenna, A. M.; Purcell, J. M.; Rodgers, R. P.; Xian, F. Petroleomics: A Test Bed for Ultrahigh-Resolution Fourier Transform Ion Cyclotron Resonance Mass Spectrometry. *Eur. J. Mass Spectrom.* **2010**, *16*, 367−371.

(71) Xian, F.; Corilo, Y. E.; Hendrickson, C. L.; Marshall, A. G. Baseline correction of absorption-mode Fourier transform ion cyclotron resonance mass spectra. *Int. J. Mass Spectrom.* **2012**, *325−327*, 67−72.

(72) Xian, F.; Hendrickson, C. L.; Blakney, G. T.; Beu, S. C.; Marshall, A. G. Automated Broadband Phase Correction of Fourier Transform Ion Cyclotron Resonance Mass Spectra. *Anal. Chem.* **2010**, *82* (21), 8807−8812.

(73) Boduszynski, M. M. Composition of heavy petroleums. 1. Molecular weight, hydrogen deficiency, and heteroatom concentration as a function of atmospheric equivalent boiling point up to 1400. degree. F (760. degree. C). *Energy Fuels* **1987**, *1* (1), 2−11.

(74) Boduszynski, M. M. Composition of heavy petroleums. 2. Molecular characterization. *Energy Fuels* **1988**, *2* (5), 597−613.

(75) Boduszynski, M. M.; Altgelt, K. H. Composition of Heavy Petroleums 0.4. Significance of the Extended Atmospheric Equivalent Boiling-Point (Aebp) Scale. *Energy Fuels* **1992**, *6* (1), 72−76.

(76) Purcell, J. M.; Hendrickson, C. L.; Rodgers, R. P.; Marshall, A. G. Atmospheric Pressure Photoionization Fourier Transform Ion Cyclotron Resonance Mass Spectrometry for Complex Mixture Analysis. *Anal. Chem.* **2006**, *78* (16), 5906−5912.

(77) Purcell, J. M.; Hendrickson, C. L.; Rodgers, R. P.; Marshall, A. G. Atmospheric pressure photoionization proton transfer for complex organic mixtures investigated by Fourier transform ion cyclotron resonance mass spectrometry. *J. Am. Soc. Mass Spectrom.* **2007**, *18* (9), 1682−1689.

(78) McLafferty, F. W.; Turecek, F. *Interpretation of Mass Spectra*, 4th ed.; University Science Books: Mill Valley, CA, 1993.

(79) Hsu, C. S.; Lobodin, V. V.; Rodgers, R. P.; McKenna, A. M.; Marshall, A. G. Compositional boundaries for fossil hydrocarbons. *Energy Fuels* **2011**, *25* (5), 2174−2178.

(80) Lobodin, V. V.; Marshall, A. G.; Hsu, C. S. Compositional space boundaries for organic compounds. *Anal. Chem.* **2012**, *84* (7), 3410−3416.

(81) Koolen, H. H.; Swarthout, R. F.; Nelson, R. K.; Chen, H.; Krajewski, L. C.; Aeppli, C.; McKenna, A. M.; Rodgers, R. P.; Reddy, C. M. Unprecedented insights into the chemical complexity of coal tar from comprehensive two-dimensional gas chromatography mass spectrometry and direct infusion Fourier transform ion cyclotron resonance mass spectrometry. *Energy Fuels* **2015**, *29* (2), 641−648.

(82) Altgelt, K. H.; Boduszynski, M. M. Composition of heavy petroleums. 3. An improved boiling point-molecular weight relation. *Energy Fuels* **1992**, *6* (1), 68−72.

(83) Stanford, L. A.; Kim, S.; Klein, G. C.; Smith, D. F.; Rodgers, R. P.; Marshall, A. G. Identification of Water-Soluble Heavy Crude Oil Organics. Acidic and Basic NSO Compounds in Fresh Water and Sea Water by Electrospray Ionization Fourier Transform Ion Cyclotron Resonance Mass Spectrometry. *Environ. Sci. Technol.* **2007**, *41*, 2696−2702.

(84) Hughey, C. A.; Minardi, C. S.; Galasso-Roth, S. A.; B, P. G.; Mapolelo, M. M.; Rodgers, R. P.; Marshall, A. G.; Ruderman, D. L. Napthenic acids as indicators of crude oil biodegradation in soil based on semi-quantitative electrospray ionization Fourier transform ion cyclotron resonance mass spectrometry. *Rapid Commun. Mass Spectrom.* **2008**, *22*, 3968−3976.

(85) Headley, J. V.; Peru, K. M.; Armstrong, S.; Han, X.; Martin, J. W.; Mapolelo, M. M.; Smith, D. F.; Rogers, R. P.; Marshall, A. G. Comparison of Aquatic Plant Derived Changes in Aqueous Naphthenic Acid Profiles Determined by ESI/MS, HPLC/QTOF MS and FT-ICR MS. *Rapid Commun. Mass Spectrom.* **2009**, *23*, 515−522.

(86) Headley, J. V.; Peru, K. M.; Armstrong, S. A.; Han, X.; Martin, J. W.; Mapolelo, M. M.; Smith, D. F.; Rogers, R. P.; Marshall, A. G. Aquatic plant-derived changes in oil sand naphthenic acid signatures determined by low-. high-and ultrahigh-resolution mass spectrometry. *Rapid Commun. Mass Spectrom.* **2009**, *23* (4), 515−522.

(87) Headley, J. V.; Peru, K. M.; Barrow, M. P. Mass spectrometric characterization of naphthenic acids in environmental samples: a review. *Mass Spectrom. Rev.* **2009**, *28* (1), 121−134.

(88) Rowland, S. J.; West, C. E.; Scarlett, A. G.; Jones, D.; Frank, R. A. Identification of indivual tetra-and pentacyclic naphthenic acids in oil sands process water by comprehensive two-dimensional gas chromatography/mass spectrometry. *Rapid Commun. Mass Spectrom.* **2011**, *25* (9), 1198−1204.

(89) Grewer, D. M.; Young, R. F.; Whittal, R. M.; Fedorak, P. M. Naphthenic acids and other acid-extractables in water samples from Alberta: What is being measured? *Sci. Total Environ.* **2010**, *408* (23), 5997−6010.

(90) Fenn, J. B.; Yamashita, M. Electrospray ion source. Another variation of the free-jet theme. *J. Phys. Chem.* **1984**, *88* (20), 4451−4459.

(91) Zhan, D. L.; Fenn, J. B. Electrospray mass spectrometry of fossil fuels. *Int. J. Mass Spectrom.* **2000**, *194* (2−3), 197−208.

(92) Lobodin, V. V.; Juyal, P.; McKenna, A. M.; Rodgers, R. P.; Marshall, A. G. Tetramethylammonium Hydroxide as a reagent for complex mixture analysis by negative ion electrospray ionization mass spectrometry. *Anal. Chem.* **2013**, *85*, 7803−7808.

(93) Zeuthen, P.; Knudsen, K. G.; Whitehurst, D. D. Organic nitrogen compounds in gas oil blends, their hydrotreated products and the importance to hydrotreatment. *Catal. Today* **2001**, *65*, 307−314.

(94) Wiwel, P.; Knudsen, K.; Zeuthen, P.; Whitehurst, D. Assessing compositional changes of nitroge compounds during hydrotreating of typical diesel range gas oils using a novel preconcentration technique coupled with gas chromatography and atomic emission detection. *Ind. Eng. Chem. Res.* **2000**, *39* (2), 533−540.

(95) Wiwel, P.; Hinnemann, B.; Hidalgo-Vivas, A.; Zeuthen, P.; Petersen, B. O.; Duus, J. Ø. Characterization and identification of the most refractory nitrogen compounds in hydroprocessed vacuum gas oil. *Ind. Eng. Chem. Res.* **2010**, *49* (7), 3184−3193.

DOI: 10.1021/acs.energyfuels.7b03944
Energy Fuels 2018, 32, 3232−3242